Theory of Umklapp-assisted recombination of bound excitons in Si:P

2009 J. Phys.: Condens. Matter 21 084218

(http://iopscience.iop.org/0953-8984/21/8/084218)

IOP PUBLISHING JOURNAL OF PHYSICS: CONDENSED MATTER

J. Phys.: Condens. Matter **21** (2009) 084218 (9pp) doi:10.1088/0953-8984/21/8/084218

Theory of Umklapp-assisted recombination of bound excitons in Si:P

Michael N Leuenberger and L J Sham

Department of Physics, University of California San Diego, La Jolla, CA 92093, USA

Received 11 August 2008, in final form 16 October 2008
Published 30 January 2009
Online at stacks.iop.org/JPhysCM/21/084218

Abstract

We present calculations for the oscillator strength of the recombination of excitons bound to phosphorus donors in silicon. We show that the direct recombination of the bound exciton cannot account for the experimentally measured oscillator strength of the no-phonon line. Instead, the recombination process is assisted by an Umklapp process of the donor electron state. We make use of the empirical pseudopotential method to evaluate the Umklapp-assisted recombination matrix element in second-order perturbation theory. Our result is in good agreement with experiment. Being potentially useful for quantum computing, the process of Umklapp-assisted recombination can be used to detect optically the spin state of the nucleus of a phosphorus donor, which requires that the energy levels of the nuclear spin are optically resolvable. We therefore present two methods to improve the optical resolution of the optical detection of the spin state of a single nucleus in Si:P.

1. Introduction

Proposals on quantum computing in semiconductors have recently attracted a great deal of attention [1, 2]. The main idea is to use the electron spin of quantum dots in semiconductors [3] or the nuclear spin of shallow donors in silicon [4] as a qubit for quantum information processing. A complete quantum computation consists of, besides the single- and two-qubit operations, the initialization and the readout of the qubits. While the initialization and the readout of the electron spin in quantum dots have been successfully demonstrated experimentally [5, 6], it remains an experimental challenge to read out the nuclear spin of a donor in silicon.

It has recently been proposed that the photoluminescence of excitons bound to phosphorus donors can be used to detect the spin state of a single donor nucleus in silicon [7]. This scheme for optical readout could render the recent quantum computing proposal using conditional NMR and ESR pulses feasible [9, 10]. Although experiments have shown that the recombination of the bound exciton follows strong optical selection rules [11], it has been unclear what physical process is responsible for the no-phonon line of the optical recombination of the bound exciton. In contrast to the phonon-assisted recombination, the no-phonon line represents the recombination process without phonon assistance. A shell model that accounts for the selection rules was proposed in [12]. The shell model was later improved in [13, 14] by a Hartree–Fock calculation that takes the multivalley character of indirect bandgap semiconductors into account and is therefore in good agreement with the measured fine-structure excitation spectrum of the bound exciton complex [15]. The Hartree–Fock calculation fails to predict binding energies. This problem was overcome by a density-functional calculation that takes the correlation energy into account [16]. However, neither model gives a satisfactory physical description of the recombination process for the no-phonon line and is thus unable to quantitatively reproduce the measured oscillator strength f_{exp} in [17]. Our calculations show that the probability for direct recombination of the bound exciton is negligibly small. Here we present a physical model of the recombination process that accurately reproduces the oscillator strength f_{exp} of the no-phonon line. In our model the recombination of the exciton is assisted by the Umklapp process of the donor electron. In section 2 we give a detailed description of our model. In section 3 we perform a Hartree approximation to calculate the envelope functions of the trion state of the two electrons and the hole. The Coulomb interaction of the two electrons and the recombination of one of the electrons with the hole are computed in section 4. For the evaluation of the recombination matrix element, we make use of the empirical pseudopotential method [18–20] to calculate the bandstructure of silicon with 137 reciprocal lattice vectors at 100 points inside the first Brillouin zone in the X direction. This technique is reviewed in appendix A. Then we use the resulting Bloch states to calculate the oscillator strength of the Umklapp-assisted recombination in second-order perturbation theory,

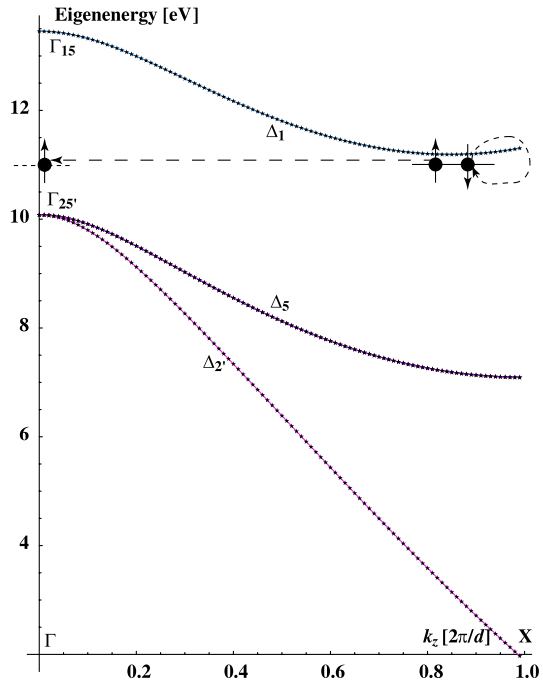

Figure 1. Bandstructure of silicon in the direction of the X point. The minimum of the conduction band with Δ_1 symmetry is located at $k_z = k_0 = 0.85k_{\mathrm{si}}$. Due to the Coulomb interaction the donor electron experiences an Umklapp process, whereas the electron of the bound exciton is virtually excited into the conduction band with an energy mismatch of $E_{\mathrm{donor}} - E_{\mathrm{c}}(k_{\mathrm{u}})$.

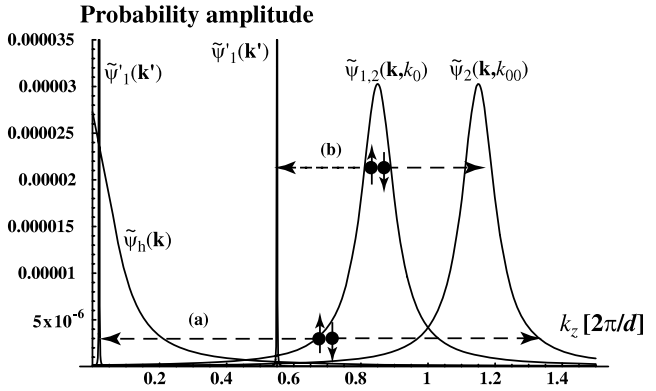

Figure 2. Before the Coulomb interaction both electrons can be described by the broad Gaussian wavefunction at $k_z = 0.85k_{\mathrm{si}}$, which represents the initial wavefunction for both electrons. After the Coulomb interaction the final state of electron 2 is represented by the broad Gaussian wavefunction at $k_z = 1.15k_{\mathrm{si}} = -0.85k_{\mathrm{si}}$ (modulo k_{si}), whereas the final state of electron 1 is virtually excited into the conduction band and can therefore be described by a narrow delta-peaked wavefunction with wavevector k_{u}. Since the Coulomb interaction conserves the total momentum of both electrons (see equation (22)), the transition amplitude M_{C} in equation (21) contains an integral over all the momentum space with scattering momenta for electrons 1 and 2 that are equal in magnitude. Therefore the arrows in the interaction processes (a) and (b) have the same length. This integral in M_{C} can be seen as a sum over interaction processes, such as (a) and (b). As figure 3 shows, the Coulomb interaction amplitude M_{C} has a maximum at $k_{\mathrm{u}} = 0.55k_{\mathrm{si}}$ due to the interaction process (b), where the final state of electron 2 has a maximum overlap with the Umklapp-scattered bound state $\tilde{\psi}_2(\mathbf{k}, k_{00})$. However, the largest contribution to the Umklapp-assisted recombination, i.e. to the integral in M_{r} in equation (26), comes from the interaction process (a), because the overlap of the virtually excited electron 1 and the hole is largest around $k_{\mathrm{u}} = 0$ (see figure 4). In order to obtain the full recombination amplitude, we have to sum over all the virtually excited states $|k_{\mathrm{u}}\rangle$ of the scattered electron. Note that this momentum-conserving interaction is allowed because of the broad distribution of the bound states at $k_z = 0.85k_{\mathrm{si}}$.

which is shown in section 5. In section 6, as an application of our model, we present two methods based on optically detected magnetic resonance (ODMR) to improve the resolution of the readout of a nuclear spin of a donor electron in silicon.

2. Physical model

In a typical photoluminescence experiment a laser with frequency well above the direct bandgap of silicon $E_{\mathrm{directgap}} = 3.4$ eV produces electron–hole pairs [11]. The excited electrons relax via electron–phonon interaction to the minima of the conduction band, which lie at the six wavevectors $\pm\mathbf{k}_{x0} = (\pm k_0, 0, 0)$, $\pm\mathbf{k}_{y0} = (0, \pm k_0, 0)$ and $\pm\mathbf{k}_{z0} = (0, 0, \pm k_0)$ with $k_0 = 0.85k_{\mathrm{si}}$ in the first Brillouin zone. $k_{\mathrm{si}} = 2\pi/d$ is the wavevector at the X point of the reciprocal lattice of silicon, which has a lattice constant of $d = 5.43$ Å. After this relaxation process the exciton gets bound to the phosphorus donor. The electron of the bound exciton and the donor electron form a spin singlet state. Then one of the two electrons recombines with the hole by emitting a photon, which is detected in the photoluminescence. In our physical model this recombination process is assisted by the Coulomb interaction of the two electrons, whereby one of them experiences an Umklapp process and the other one is virtually excited into the conduction band with momentum k_{u} and energy $E_{\mathrm{c}}(k_{\mathrm{u}})$ (see figure 1). In other words, the Coulomb interaction of the two electrons in the case of the no-phonon line plays the role of the phonon assistance in the case of the single-phonon line. Due to the Coulomb exchange interaction they prefer to stay in the same valley. We start with the entangled two-electron six-valley symmetric ground state $|\mathbf{k}_{x0}\rangle_1|\mathbf{k}_{x0}\rangle_2 + |-\mathbf{k}_{x0}\rangle_1|-\mathbf{k}_{x0}\rangle_2 + |\mathbf{k}_{y0}\rangle_1|\mathbf{k}_{y0}\rangle_2 + |-\mathbf{k}_{y0}\rangle_1|-\mathbf{k}_{y0}\rangle_2 + |\mathbf{k}_{z0}\rangle_1|\mathbf{k}_{z0}\rangle_2 + |-\mathbf{k}_{z0}\rangle_1|-\mathbf{k}_{z0}\rangle_2$. The Coulomb interaction has its maximum amplitude if the final state is $|-\mathbf{k}_{x0}\rangle_1|\mathbf{k}_{xu0}\rangle_2 + |\mathbf{k}_{x0}\rangle_1|-\mathbf{k}_{xu0}\rangle_2 + |-\mathbf{k}_{y0}\rangle_1|\mathbf{k}_{yu0}\rangle_2 + |\mathbf{k}_{y0}\rangle_1|-\mathbf{k}_{yu0}\rangle_2 + |-\mathbf{k}_{z0}\rangle_1|\mathbf{k}_{zu0}\rangle_2 + |\mathbf{k}_{z0}\rangle_1|-\mathbf{k}_{zu0}\rangle_2$ (see process (b) in figure 2). Electron 1 gets scattered onto itself, because $k_0 + 0.3k_{\mathrm{si}} = -k_0$ (modulo k_{si}) in the first Brillouin zone. Due to momentum conservation we get $\pm\mathbf{k}_{xu0} = (\pm k_{\mathrm{u}0}, 0, 0)$, $\pm\mathbf{k}_{yu0} = (0, \pm k_{\mathrm{u}0}, 0)$, and $\pm\mathbf{k}_{zu0} = (0, 0, \pm k_{\mathrm{u}0})$ with $k_{\mathrm{u}0} = 0.55k_{\mathrm{si}} = k_0 - 0.3k_{\mathrm{si}}$. While the initial and the final state of electron 1 are bound states of broad Gaussian shape in k-space, the initial state of electron 2 is a bound state of broad Gaussian shape and the final state is a free state of narrow delta-peak shape, as is shown in figure 2. Although the Coulomb interaction is strongest for process (b) in figure 2, the recombination amplitude is rather small at $k_{\mathrm{u}} = k_{\mathrm{u}0} = 0.55k_{\mathrm{si}}$. This means that interaction processes with $k_{\mathrm{u}} > k_{\mathrm{u}0}$ can be safely neglected. It turns out that the largest contribution to the Umklapp-assisted recombination comes from the continuum of

scattered states around $k_u = 0$, which is depicted by process (a) in figure 2. The reason for this is that the hole of the bound exciton is centered at the maximum of the valence band at $\mathbf{k} = 0$.

In order to calculate the Coulomb interaction between the two electrons and the recombination of one of the two electrons with the hole, we need to compute their envelope wavefunctions (see figure 2) and their Bloch wavefunctions. The envelope of the trion state of two electrons and one hole bound to the phosphorus impurity is computed in the Hartree approximation, which allows us to represent the trion state by single-particle wavefunctions of the two electrons and the hole. The Bloch wavefunctions are computed by means of the empirical pseudopotential method (see appendix B). For the Coulomb interaction between the trion state and the scattered state, we consider only the Coulomb interaction between the two electrons. Both the Coulomb interaction and also the recombination of one of the electrons with the hole are computed in **k**-space. Our goal is to calculate the transition amplitude of the Umklapp-assisted recombination in second-order perturbation theory, which is described by

$$M_{\rm tot} = \sum_{j=\pm x,\pm y,\pm z} \frac{1}{6k_0} \int_0^{k_0} {\rm d}k_{\rm u} \frac{M_{\rm r} M_{\rm C}}{E_{\rm donor} - E_{\rm c}(k_{\rm u})}, \qquad (1)$$

where we use the notation $\mathbf{k}_{\pm x0} = \pm\mathbf{k}_{x0}$, $\mathbf{k}_{\pm y0} = \pm\mathbf{k}_{y0}$, and $\mathbf{k}_{\pm z0} = \pm\mathbf{k}_{z0}$. $E_{\rm donor}$ is the energy level of the donor electron and $E_{\rm c}(k_{\rm u})$ is the energy of the conduction band. The Coulomb matrix element is given by

$$M_{\rm C} = \left\langle \psi_1'(\mathbf{k}_{ju})\psi_2'(-\mathbf{k}_{j0})\psi_{\rm h}(0)\,|V_{\rm C}|\,\psi_1(\mathbf{k}_{j0})\psi_2(\mathbf{k}_{j0})\psi_{\rm h}(0)\right\rangle, \qquad (2)$$

and the recombination matrix element by

$$M_{\rm r} = \left\langle \psi_2'(-\mathbf{k}_{j0})\,|V_{\rm r}|\,\psi_1'(\mathbf{k}_{ju})\psi_2'(-\mathbf{k}_{j0})\psi_{\rm h}(0)\right\rangle. \qquad (3)$$

The Umklapp assistance becomes obvious when looking at electron 2 that makes a transition from $\psi_2(\mathbf{k}_{j0})$ to $\psi_2'(-\mathbf{k}_{j0})$. Electron 1 with wavevector $\mathbf{k}_1$ is scattered via the Coulomb potential

$$V_{\rm C} = \frac{q^2 {\rm e}^{-r\sqrt{\xi_l^2+2\xi_t^2}}}{4\pi\epsilon r} \qquad (4)$$

off electron 2 with wavevector $\mathbf{k}_2$, thereby conserving the momenta, i.e. $\mathbf{k}_1 + \mathbf{k}_2 = \mathbf{k}_1' + \mathbf{k}_2'$. After the Umklapp process of electron 2 the virtually excited electron with wavevector $\mathbf{k}_1'$ recombines with the bound hole with wavevector $\mathbf{k}_{\rm h}' = \mathbf{k}_1'$ via the electron–photon interaction

$$V_{\rm r} = \frac{q}{m_{\rm t}} A_\perp p_\perp, \qquad (5)$$

which results in the emission of a photon that can be seen in a photoluminescence experiment. $\epsilon_0 = 8.854 \times 10^{-12}$ F m^{-1} is the dielectric constant of the vacuum, and $\epsilon_{\rm r} = 11.56$ is the relative dielectric constant of silicon, which are combined to $\epsilon = \epsilon_0\epsilon_{\rm r}$ [21]. So the refractive index of silicon is about $\nu = \sqrt{\epsilon_{\rm r}} = 3.4$. $\xi_l = 4m_{\rm l}k_{\rm F}q^2/\pi\hbar^2 = 1.9 \times 10^9$ m^{-1} and $\xi_t = 4m_{\rm t}k_{\rm F}q^2/\pi\hbar^2 = 4.0 \times 10^8$ m^{-1} are the Thomas–Fermi screening lengths in longitudinal and transverse directions, where $k_{\rm F} = (3\pi^2 n_0)^{1/3}$ is the Fermi wavevector and $n_0 = 1/L^3$ is the density of the donor electrons [22]. The distance between the donor electrons is about $L = 4$ nm [23]. The longitudinal mass in silicon is $m_{\rm l} = 0.9163m_{\rm e}$, where $m_{\rm e} = 9.1095 \times 10^{-31}$ kg is the bare electron mass. The transverse mass in silicon is $m_{\rm t} = 0.1905m_{\rm e}$.

3. Hartree approximation

Let us start by analyzing the initial state of the trion. Due to the Coulomb exchange interaction the two electrons are in a spin singlet state $(|\uparrow_1\downarrow_2\rangle - |\downarrow_1\uparrow_2\rangle)/\sqrt{2}$, and their orbital wavefunction is symmetric in the valley combinations, i.e.

$$\psi_{12} = \frac{1}{\sqrt{6}} \sum_{j=\pm x0,\pm y0,\pm z0} F_{1\mathbf{k}_j}\phi_{1\mathbf{k}_j} F_{2\mathbf{k}_j}\phi_{2\mathbf{k}_j}. \qquad (6)$$

For the Hartree approximation the envelope function of a bound electron is chosen to be

$$F_{\mathbf{ek}_{z0}}(\mathbf{r}) = F_{1\mathbf{k}_{z0}}(\mathbf{r}) = F_{2\mathbf{k}_{z0}}(\mathbf{r}) = \frac{1}{\sqrt{a^2 b}} {\rm e}^{-\frac{|x|+|y|}{a}} {\rm e}^{-\frac{|z|}{b}}, \qquad (7)$$

where $a = 25.1$ Å and $b = 14.4$ Å (see [24, 25]). The Bloch wavefunction of an electron is given by

$$\phi_{\mathbf{ek}_{z0}}(\mathbf{r}) = \phi_{1\mathbf{k}_{z0}}(\mathbf{r}) = \phi_{2\mathbf{k}_{z0}}(\mathbf{r}) = u_{\rm cz}(\mathbf{r}){\rm e}^{{\rm i}k_0 z}, \qquad (8)$$

where $k_0 = 0.85k_{\rm si}$ is the distance from the Γ point to the minimum of the conduction band in the X direction (see next section). The Bloch wavefunction of the hole is

$$\phi_{\rm h}(\mathbf{r}) = u_{\rm v}^*(\mathbf{r}). \qquad (9)$$

The effective Hartree potential $V_{\rm hH}(r) = V_{\rm D}(r) + 2V_{\rm e}(r)$ that is felt by the hole is a superposition of the donor potential $V_{\rm D}(r) = e/4\pi\epsilon r$ and the effective Hartree potential of the two electrons, which is determined by

$$\begin{aligned} V_{\rm e}(r) &= -\frac{e}{4\pi\epsilon}\int \frac{\left|\varphi(\mathbf{r}')\right|^2}{|\mathbf{r}'-\mathbf{r}|}{\rm d}^3r' \\ &= -\frac{e}{2\epsilon}\int_1^{-1}\int_0^{\infty} \frac{r'^2\left|\varphi(\mathbf{r}')\right|^2}{\left|\sqrt{r'^2+r^2-2rr'\cos\theta}\right|}{\rm d}r'\,{\rm d}\cos\theta \\ &= -\frac{e}{2\epsilon}\int_0^{r} \frac{r'^2\left|\varphi(\mathbf{r}')\right|^2}{r}{\rm d}r' - \frac{e}{2\epsilon}\int_r^{\infty} r'\left|\varphi(\mathbf{r}')\right|^2{\rm d}r'. \end{aligned} \qquad (10)$$

Only for evaluation of $V_{\rm e}(r)$ we approximate the electron envelope wavefunctions by

$$\varphi(r') = \frac{{\rm e}^{-r'/b}}{\sqrt{\pi}a_{\rm opt}^{3/2}}, \qquad (11)$$

where $a_{\rm opt} = (2a+b)/3$. The electron envelope wavefunction looks like a hydrogen wavefunction for $n = 1$ and $l = 0$. Then we obtain

$$V_{\rm hH}(r) = \frac{e}{4\pi\epsilon r}\left[-1 + 2\left(1 + \frac{r}{a_{\rm opt}}\right){\rm e}^{-2r/a_{\rm opt}}\right], \qquad (12)$$

which is shown in figure 5. Solving numerically for the ground state of $V_{\rm hH}(r)$ by means of the finite difference method leads to a binding energy of -0.02 eV. The envelope wavefunction of the bound hole can be well approximated by

$$F_{\rm h}(r) = \left(\frac{1}{2c}\right)^{5/2} \frac{r}{\sqrt{3\pi}} {\rm e}^{-\frac{r}{2c}}, \tag{13}$$

where $c = 20$ Å. The hole envelope wavefunction looks like a hydrogen wavefunction for $n = 2$ and $l = 1$.

For self-consistency we also calculate the effective Hartree potential $V_{\rm eH}(r) = V_{\rm D}(r) + V_{\rm e}(r) + V_{\rm h}(r)$ that is felt by one of the two electrons, for which we obtain

$$V_{\rm eH}(r) = \frac{e}{4\pi\epsilon r}\left[1 + \left(1 + \frac{r}{a_{\rm opt}}\right){\rm e}^{-2r/a_{\rm opt}} - \left(1 + \frac{3r}{4c} + \frac{r^2}{4c^2} + \frac{r^3}{24c^3}\right){\rm e}^{-r/c}\right]. \tag{14}$$

The ground state of the bound electron is well approximated by equation (11) with $a_{\rm opt} \approx (2a + b)/3 = 21.5$ Å. Thus our values for $a_{\rm opt}$ and c are self-consistent.

4. Coulomb and recombination matrix elements

We are going to calculate the matrix elements $M_{\rm C}$ and $M_{\rm r}$ in the reciprocal lattice space by Fourier transforming the wavefunctions. The Bloch wavefunctions can be expanded in reciprocal lattice vectors as

$$\phi_{{\rm e}\mathbf{k}_{z0}}(\mathbf{r}) = {\rm e}^{{\rm i}k_{z0}z} \sum_{\mathbf{G}} u_{c\mathbf{G}} {\rm e}^{{\rm i}\mathbf{G}\cdot\mathbf{r}} \tag{15}$$

for the electron wavefunctions and

$$\phi_{\rm h}(\mathbf{r}) = \sum_{\mathbf{G}} u^*_{v\mathbf{G}} {\rm e}^{-{\rm i}\mathbf{G}\cdot\mathbf{r}} \tag{16}$$

for the hole wavefunction. Thus the electron wavefunctions in $\mathbf{k}$-space are given by $\tilde{\psi}_{\rm e}(\mathbf{k}, k_{\rm c}) = \sum_{\mathbf{G}} u_{c\mathbf{G}} \tilde{\psi}_{{\rm e}\mathbf{G}}(\mathbf{k}, k_{\rm c})$ with

$$\tilde{\psi}_{{\rm e}\mathbf{G}}(\mathbf{k}, k_{\rm c}) = \left(\frac{2}{\pi a^2 b}\right)^{\frac{3}{2}} \frac{1}{\left(\frac{1}{a^2} + (k_x + G_x)^2\right)} \times \frac{1}{\left(\frac{1}{a^2} + (k_y + G_y)^2\right)} \frac{1}{\left(\frac{1}{b^2} + (k_z + G_z - k_{\rm c})^2\right)}, \tag{17}$$

centered at $k_{\rm c}$. For simple Fourier transformation in Cartesian coordinates we approximate the hole envelope wavefunction by

$$F_{\rm h}(\mathbf{r}) = \left(\frac{1}{2c}\right)^{5/2} \frac{|x| + |y| + |z|}{\sqrt{3}} {\rm e}^{-\frac{|x|+|y|+|z|}{2c}}. \tag{18}$$

The hole wavefunction is then well approximated by $\tilde{\psi}_{\rm h}(\mathbf{k}) = \sum_{\mathbf{G}} u^*_{v\mathbf{G}} \tilde{\psi}_{{\rm h}\mathbf{G}}(\mathbf{k})$ with

$$\tilde{\psi}_{{\rm h}\mathbf{G}}(\mathbf{k}) = \left(\frac{2}{\pi(2c)^3}\right)^{\frac{3}{2}} \frac{1}{\left(\frac{1}{(2c)^2} + (k_x - G_x)^2\right)} \times \frac{1}{\left(\frac{1}{(2c)^2} + (k_y - G_y)^2\right)} \frac{1}{\left(\frac{1}{(2c)^2} + (k_z - G_z)^2\right)}. \tag{19}$$

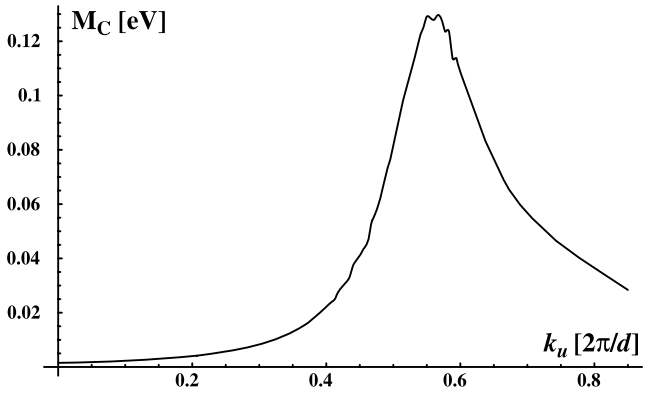

Figure 3. The Coulomb interaction amplitude $M_{\rm C}$ in equation (21) between the electron of the bound exciton and the donor electron has a maximum at $k_{\rm u} = 0.55k_{\rm si}$.

So the initial wavefunctions of the two electrons are $\tilde{\psi}_1(\mathbf{k}) = \tilde{\psi}_2(\mathbf{k}) = \tilde{\psi}_{\rm e}(\mathbf{k}, k_{\rm c} = k_0)$. The wavefunction of the virtually excited electron in $\mathbf{k}$-space is given by $\tilde{\psi}'_1(\mathbf{k}') = \sum_{\mathbf{G}} u_{c\mathbf{G}} \tilde{\psi}_{1\mathbf{G}}(\mathbf{k}')$ with

$$\tilde{\psi}_{1\mathbf{G}}(\mathbf{k}') = \left(\frac{2}{\pi a^2 b}\right)^{\frac{3}{2}} \frac{1}{\left(\frac{1}{a_u^2} + (k_x + G_x)^2\right)} \times \frac{1}{\left(\frac{1}{a_u^2} + (k_y + G_y)^2\right)} \frac{1}{\left(\frac{1}{a_u^2} + (k_z + G_z - k_{\rm u})^2\right)}, \tag{20}$$

where $a_u = 1000d$. The wavefunction of the Umklapp-scattered electron 2 is given by $\tilde{\psi}'_2(\mathbf{k}') = \tilde{\psi}_{\rm e}(\mathbf{k}, k_{\rm c} = k_{00})$, where $k_{00} = 1.15k_{\rm si}$, and the intermediate hole wavefunction by $\tilde{\psi}'_{\rm h}(\mathbf{k}') = \tilde{\psi}_{\rm h}(\mathbf{k})$. Note that only the two electrons scatter off each other.

Since the Coulomb interaction is local within each Brillouin zone, interference effects can be neglected and thus it is sufficient to calculate the Coulomb interaction matrix element within the first Brillouin zone, i.e.

$$M_{\rm C} = \langle \psi'_1 \psi'_2 | V_{\rm C} | \psi_1 \psi_2 \rangle = \frac{q^2}{\epsilon} \int {\rm d}^3k'_1 \int {\rm d}^3k_1 \int {\rm d}^3k_2 \times \tilde{\psi}'^*_{10}(\mathbf{k}'_1) \tilde{\psi}'^*_{20}(\mathbf{k}_1 - \mathbf{k}'_1 + \mathbf{k}_2) \frac{1}{\left(\mathbf{k}_1 - \mathbf{k}'_1\right)^2 + \xi^2} \times \tilde{\psi}_{10}(\mathbf{k}_1) \tilde{\psi}_{20}(\mathbf{k}_2), \tag{21}$$

where we used the relation

$$\int {\rm d}^3r_1 \int {\rm d}^3r_2 {\rm e}^{-{\rm i}\mathbf{k}'_1\cdot\mathbf{r}_1} {\rm e}^{-{\rm i}\mathbf{k}'_2\cdot\mathbf{r}_2} \frac{q^2 {\rm e}^{-\xi r_{12}}}{4\pi\epsilon r_{12}} {\rm e}^{{\rm i}\mathbf{k}_1\cdot\mathbf{r}_1} {\rm e}^{{\rm i}\mathbf{k}_2\cdot\mathbf{r}_2} = \frac{q^2}{(2\pi)^3\epsilon} \int {\rm d}^3k_{12} \frac{\delta(\mathbf{k}_1 - \mathbf{k}'_1 + \mathbf{k}_{12})\delta(\mathbf{k}_2 - \mathbf{k}'_2 - \mathbf{k}_{12})}{k_{12}^2 + \xi^2} = \frac{q^2}{(2\pi)^3\epsilon} \frac{1}{\left(\mathbf{k}_1 - \mathbf{k}'_2\right)^2 + \xi^2} \delta(\mathbf{k}_1 - \mathbf{k}'_1 + \mathbf{k}_2 - \mathbf{k}'_2), \tag{22}$$

where $\mathbf{r}_{12} = \mathbf{r}_1 - \mathbf{r}_2$ and $\mathbf{k}_{12} = 2\pi/\mathbf{r}_{12}$. M_C is plotted in figure 3. Note that there is no $\sqrt{2}$ term in equation (21), because the bound hole, being in a specific spin state, chooses only one spin state out of the singlet state. So only the bright exciton recombines. The dark exciton cannot recombine.

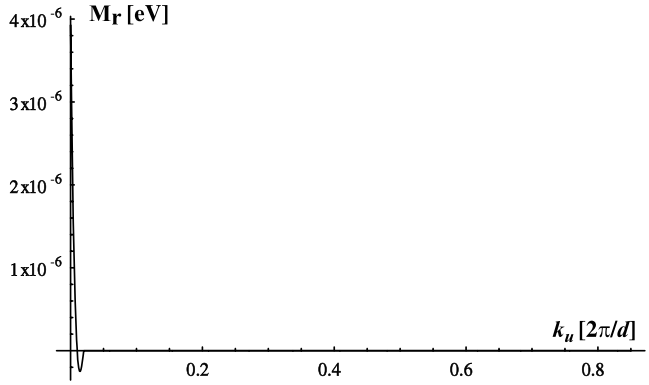

Figure 4. The recombination amplitude M_r in equation (26) for the unbound scattered electron is largest around $k_\mathrm{u} = 0$.

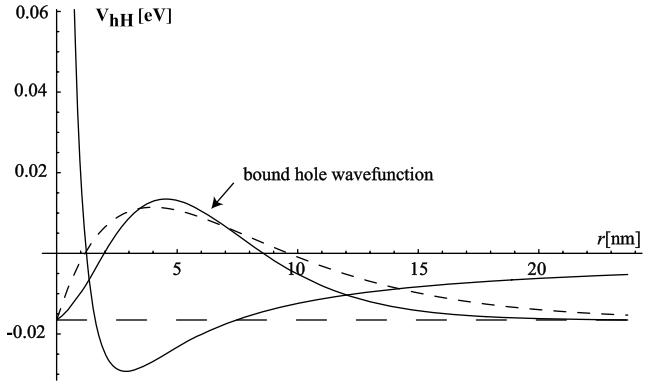

Figure 5. The effective Hartree potential produced by the donor and the two electrons. The hole wavefunction is bound in the ground state with a binding energy of −0.02 eV. The solid wavefunction was calculated by means of the finite difference method. The dashed wavefunction is given in equation (13).

Numerical calculations show that the Coulomb potential is well approximated by

$$\tilde{V}_\mathrm{C}(\mathbf{k}_1 - \mathbf{k}_1') \approx \frac{q^2}{\epsilon} \frac{1}{\left(k_{1z} - k_{1z}'\right)^2 + \xi^2}, \tag{23}$$

i.e. only the longitudinal dependence of the Coulomb potential in the z direction is taken into account. The reason for this good approximation is that the conduction band at $k_z = k_0$ is much flatter in the longitudinal direction than in the transverse direction, which means that the wavefunctions of the bound electrons are broad in the longitudinal direction but narrow in the transverse direction. This is also reflected by the difference in effective longitudinal and transverse masses, $m_\mathrm{l} = 0.9163 m_\mathrm{e}$ and $m_\mathrm{t} = 0.1905 m_\mathrm{e}$, respectively. Then the integrations in x and y directions can be solved analytically, which yields

$$\begin{aligned} M_\mathrm{C} = \tau_\perp^2 \frac{q^2}{\epsilon} \int \mathrm{d}k_{1z}' \int \mathrm{d}k_{1z} \int \mathrm{d}k_{2z} \tilde{\psi}'^*_{10}(k_{1z}') \\ \times \tilde{\psi}'^*_{20}(k_{1z} - k_{1z}' + k_{2z}) \frac{1}{\left(k_{1z} - k_{1z}'\right)^2 + \xi^2} \\ \times \tilde{\psi}_{10}(k_{1z}) \tilde{\psi}_{20}(k_{2z}), \end{aligned} \tag{24}$$

where $\tau_\perp = \frac{\pi}{a}$. Since the scattered electron state $\tilde{\psi}'^*_{10}(k_{1z}')$ is unbound, we can treat it as the square root of a delta-function with width a_u, i.e. $\tilde{\psi}'^*_{10}(k_{1z}') = \sqrt{\delta^{(a_u)}(k_{1z}' - k_\mathrm{u})}$. This means that we can approximate the integral $\int \mathrm{d}k_{1z}' \tilde{\psi}'^*_{10}(k_{1z}') h(k_{1z}')$ by $h(k_\mathrm{u})\zeta$, where $\zeta = \int \mathrm{d}k_{1z}' \tilde{\psi}'^*_{10}(k_{1z}')$, for any function $h(k_{1z}')$. Thus we obtain

$$\begin{aligned} M_\mathrm{C} = \tau_\perp^2 \zeta \frac{q^2}{\epsilon} \int \mathrm{d}k_{1z} \int \mathrm{d}k_{2z} \tilde{\psi}'^*_{20}(k_{1z} - k_\mathrm{u} + k_{2z}) \\ \times \frac{1}{(k_{1z} - k_\mathrm{u})^2 + \xi^2} \tilde{\psi}_{10}(k_{1z}) \tilde{\psi}_{20}(k_{2z}), \end{aligned} \tag{25}$$

which is solved numerically (see figure 3). The maximum of M_C is located at $k_\mathrm{u} = 0.55 k_\mathrm{si}$, which is due to the interaction process (b) shown in figure 2. In the case of the recombination we cannot neglect interference effects, because the electron–photon interaction is nonlocal in $\mathbf{k}$-space. We obtain

$$M_\mathrm{r} = \frac{\hbar q A_\perp}{m} \int \mathrm{d}^3 k_\mathrm{h}' \tilde{\psi}_\mathrm{h}'^*(\mathbf{k}_\mathrm{h}') k_{\mathrm{h}\perp}' \tilde{\psi}_\mathrm{l}'(\mathbf{k}_\mathrm{h}'), \tag{26}$$

which is solved numerically. M_r has only a single peak at $k_\mathrm{u} = 0$ with a width of about $k_0/100$.

In order to evaluate the oscillator strength, we need to calculate the bandstructure of silicon, which is reviewed in appendix A and shown in figure 1.

5. Oscillator strength

In textbooks such as [27] the oscillator strength is defined as

$$f = \frac{2}{m E_\mathrm{ni}} \left| \langle n | \, p \, | i \rangle \right|^2, \tag{27}$$

where E_ni is the energy difference between the initial $|i\rangle$ and the final state $|n\rangle$. For our Umklapp-assisted recombination the oscillator strength is thus given by

$$f_\mathrm{tot} = \frac{2}{m_\mathrm{opt} E_\mathrm{gap}} \left| \frac{g_\mathrm{hh} g_\mathrm{s} M_\mathrm{tot}}{\frac{q}{m_\mathrm{t}} A_\perp} \right|^2, \tag{28}$$

where $E_\mathrm{gap} = 1.1$ eV is the indirect bandgap energy, $m_\mathrm{opt} = 3/(1/m_\mathrm{l} + 2/m_\mathrm{t})$ is the effective mass of the electron that ensures the sum rule $\sum_n f_\mathrm{ni} = 1$ [28], $g_\mathrm{hh} = 2$ is the degeneracy of the heavy-hole band and $g_\mathrm{s} = 2$ is the spin degeneracy. We calculate first numerically the Coulomb interaction amplitude $M_\mathrm{C}(k_\mathrm{u})$, which is shown in figure 3. Then we calculate numerically the recombination amplitude $M_\mathrm{r}(k_\mathrm{u})$. Inserting $M_\mathrm{C}(k_\mathrm{u})$ and $M_\mathrm{r}(k_\mathrm{u})$ into equation (1) and integrating over k_u yields

$$f_\mathrm{tot} = 1.3 \times 10^{-6}, \tag{29}$$

which is in good agreement with the oscillator strength $f_\mathrm{exp} = 7.1 \times 10^{-6}$ of the recombination of an exciton bound to a phosphorus donor in silicon reported in [17]. Our calculation is very robust, because all our approximations are controlled. For example, deviations of 1% of the width of the Gaussian wavefunctions of the bound electrons and the hole yield negligible changes of the resulting oscillator strength f_tot. As another example, if we change the width of the hole envelope

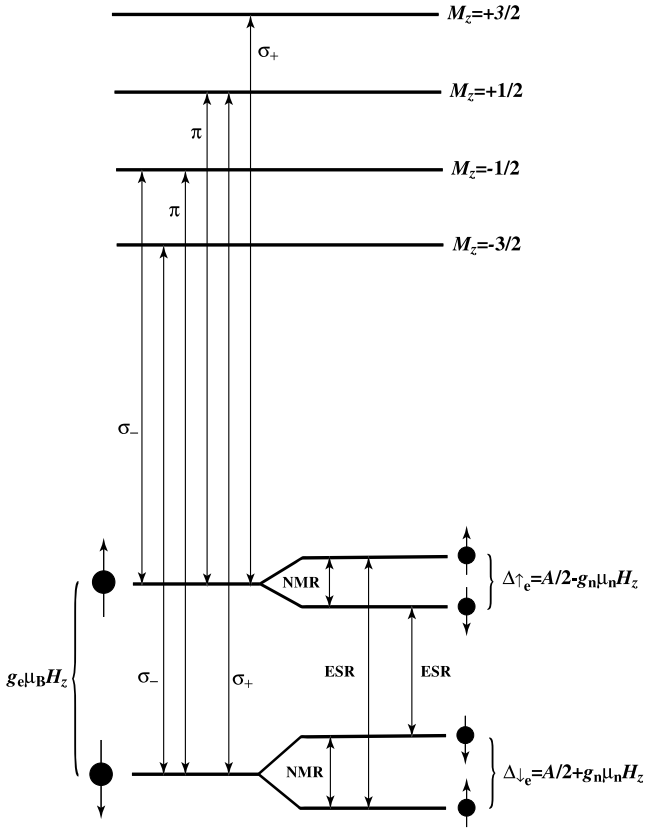

Figure 6. The energy levels of the electron and nuclear spin of the donor electron are shown at the bottom. The energy levels of the bound hole are shown at the top.

wavefunction by a factor of 10, we obtain a change in oscillator strength by a factor of about 3. For comparison, the direct recombination of the bound electron with the bound hole over the indirect bandgap has an oscillator strength of $f_{\text{direct}} = 4 \times 10^{-33}$. Thus our calculation shows that the no-phonon line in Si:P is due to the Umklapp-assisted recombination of the bound exciton. It would be interesting to check if our theory of Umklapp-assisted recombination can also account for the oscillator strengths of other donors. These calculations will be presented elsewhere.

6. Optical readout

The Umklapp-assisted recombination described in the previous sections follows strong optical selection rules, as shown in appendix A. Therefore it can be used to detect the spin state of a single nucleus in the phosphorus donor, provided that the laser produces excitons continuously that can bind to the single phosphorus impurity. The small amount of photoluminescence is then compensated by a time ensemble of measurements. The basic scheme for this optical detection of the nuclear spin was presented in [7]. However, one major obstacle that was not addressed in [7] is the bad optical resolution of the Umklapp-assisted recombination process, which makes the nuclear spin readout impossible. In this section we show two methods that can be used to improve the optical resolution such that the optical detection of the spin state of a single nucleus becomes possible. The first method is inspired by the optically detected magnetic resonance technique (ODMR) [8], where the Rabi oscillation that is induced by electron spin resonance (ESR) alters the lifetime of the bound exciton and is thus optically detectable. Since the transition from the bound hole state $M_J = -3/2$ to $M_S = +1/2$ is forbidden, mixing the spin states in an equal superposition of $M_S = +1/2$ and $M_S = -1/2$ by means of the ESR field leads to a doubling of the lifetime of the bound exciton. The second method makes use of a strong ESR field that renormalizes the spin levels in such a way that the hyperfine and Zeeman splitting of the nuclear spin is increased. As in the first method, the photons of the ESR field dress the spin states of the donor electron.

Table 1. The hyperfine and Zeeman splitting of the spin states of the donor electron.

H_z (T)	$g_e\mu_B H_z$ (meV)	$g_n\mu_n H_z$ (μeV)	$\Delta_{\uparrow_e}$ (μeV)	$\Delta_{\downarrow_e}$ (μeV)
3.0	0.35	0.21	0.03	0.46
5.0	0.58	0.36	−0.11	0.61
7.0	0.81	0.50	−0.25	0.75

The Hamiltonian for the electron–nucleus system is

$$\mathcal{H}_s = g_e\mu_B \mathbf{H}\cdot\mathbf{S} - g_n\mu_n \mathbf{H}\cdot\mathbf{I} + A\mathbf{S}\cdot\mathbf{I} \tag{30}$$

in the generalized rotating frame. The energy levels of the electron and nuclear spin are shown in figure 6. Since we intend to apply a strong microwave field for the ESR resonance for both of our methods, we also quantize the microwave field for the following description of both of our methods, the ODMR method and the frequency-resolved measurement. Typical external magnetic fields used in experiments are $H_z = 3.0, 5.0$ and 7.0 T. In a field of $H_z = 3.0$ T the Zeeman splittings of the electron and nuclear spin are $g_e\mu_B H_z = 0.35$ meV and $g_n\mu_n H_z = 0.21$ μeV, respectively. The hyperfine splitting is $A = 0.50$ μeV. Thus the splitting between $|\uparrow_e\uparrow_n\rangle$ and $|\uparrow_e\downarrow_n\rangle$ is $\Delta_{\uparrow_e} = E_{\uparrow_e\uparrow_n} - E_{\uparrow_e\downarrow_n} = A/2 - g_n\mu_n H_z = 0.03$ μeV, whereas the splitting between $|\downarrow_e\uparrow_n\rangle$ and $|\downarrow_e\downarrow_n\rangle$ is $\Delta_{\downarrow_e} = E_{\downarrow_e\downarrow_n} - E_{\downarrow_e\uparrow_n} = A/2 + g_n\mu_n H_z = 0.46$ μeV. The hyperfine and Zeeman splittings for $H_z = 3.0, 5.0$ and 7.0 T are shown in table 1.

In order to quantize the strong microwave field, we follow here the derivation of dressed states given in [29]. The Hamiltonian of the quantized photon field is

$$\mathcal{H}_p = \hbar\omega \hat{a}^\dagger \hat{a}, \tag{31}$$

where $\hat{a}$ ($\hat{a}^\dagger$) is the annihilation (creation) operator of a photon. The interaction between the microwave photons and spin of the electron of the phosphorus donor is described by

$$V = -\boldsymbol{\mu}\cdot\mathbf{B}, \tag{32}$$

where the quantized magnetic field is given by

$$\mathbf{B} = \sqrt{\frac{\hbar}{2\epsilon_0 c_p^2 L^3}}\left[\hat{a}\frac{\mathrm{i}\,(\mathbf{k}\times\boldsymbol{\epsilon})}{k} + \hat{a}^\dagger\frac{(-\mathrm{i})\,(\mathbf{k}\times\boldsymbol{\epsilon}^*)}{k}\right], \tag{33}$$

where c_p is the light velocity. The spin–photon interaction can be simplified to

$$V = g_{\text{sp}}\left[(\mathbf{e}\cdot\mathbf{S})\,\hat{a} + \left(\mathbf{e}^*\cdot\mathbf{S}\right)\hat{a}^\dagger\right]. \tag{34}$$

We use the circular polarization vectors

$$\mathbf{e}_{\pm} = \frac{1}{\sqrt{2}}\left(\mathbf{e}_x \pm \mathrm{i}\mathbf{e}_y\right) \tag{35}$$

and the spin ladder operators $S_{\pm} = S_x \pm \mathrm{i}S_y$. Then we obtain

$$\begin{aligned} V_{\sigma^+} &= \frac{g_{\mathrm{sp}}}{\sqrt{2}}\left(\hat{a}S_+ + \hat{a}^\dagger S_-\right), \\ V_{\sigma^-} &= \frac{g_{\mathrm{sp}}}{\sqrt{2}}\left(\hat{a}S_- + \hat{a}^\dagger S_+\right). \end{aligned} \tag{36}$$

There are two coupled states

$$\begin{aligned} \left|\phi_{\downarrow_{\mathrm{e}}}\right\rangle &= \left|\downarrow_{\mathrm{e}}, N+1\right\rangle, \\ \left|\phi_{\uparrow_{\mathrm{e}}}\right\rangle &= \left|\uparrow_{\mathrm{e}}, N\right\rangle. \end{aligned} \tag{37}$$

If the interaction vanishes, the energies are $E_{\downarrow_{\mathrm{e}}} = (N+1)\hbar\omega - \frac{1}{2}\hbar\omega_0$ and $E_{\uparrow_{\mathrm{e}}} = N\hbar\omega + \frac{1}{2}\hbar\omega_0$. The energy separation is $\hbar\omega_{\downarrow_{\mathrm{e}}\uparrow_{\mathrm{e}}} = \hbar(\omega - \omega_0)$. The matrix elements of V_{σ^+} read

$$\begin{aligned} \left\langle\phi_{\downarrow_{\mathrm{e}}}\right| V_{\sigma^+} \left|\phi_{\downarrow_{\mathrm{e}}}\right\rangle &= \left\langle\phi_{\uparrow_{\mathrm{e}}}\right| V_{\sigma^+} \left|\phi_{\uparrow_{\mathrm{e}}}\right\rangle = 0, \\ \left\langle\phi_{\uparrow_{\mathrm{e}}}\right| V_{\sigma^+} \left|\phi_{\downarrow_{\mathrm{e}}}\right\rangle &= \frac{g_{\mathrm{sp}}}{\sqrt{2}}\sqrt{N+1} \approx \hbar\Omega = g_{\mathrm{sp}}\sqrt{\frac{\langle N\rangle}{2}}. \end{aligned} \tag{38}$$

The eigenstates are

$$\begin{aligned} \left|\chi_1(N)\right\rangle &= \sin\theta\left|\phi_{\downarrow_{\mathrm{e}}}\right\rangle + \cos\theta\left|\phi_{\uparrow_{\mathrm{e}}}\right\rangle, \\ \left|\chi_2(N)\right\rangle &= \cos\theta\left|\phi_{\downarrow_{\mathrm{e}}}\right\rangle - \sin\theta\left|\phi_{\uparrow_{\mathrm{e}}}\right\rangle, \end{aligned} \tag{39}$$

where $\tan 2\theta = -\Omega/(\omega - \omega_0)$, $0 \leqslant 2\theta < \pi$. The eigenenergies are

$$E_{1/2} = \left(N + \frac{1}{2}\right)\hbar\omega \pm \hbar\sqrt{\left(\frac{\omega-\omega_0}{2}\right)^2 + \left(\frac{\Omega}{2}\right)^2}. \tag{40}$$

Let us tune the oscillating transverse microwave field to the ESR transition between $|\uparrow_{\mathrm{e}}\uparrow_{\mathrm{n}}\rangle$ and $|\downarrow_{\mathrm{e}}\uparrow_{\mathrm{n}}\rangle$, which we need for both of our methods. Then the eigenstates are

$$\begin{aligned} \left|\chi_{\uparrow_{\mathrm{n}}1}\right\rangle &= \left(\left|\phi_{\downarrow_{\mathrm{e}}}\right\rangle + \left|\phi_{\uparrow_{\mathrm{e}}}\right\rangle\right)\left|\uparrow_{\mathrm{n}}\right\rangle/\sqrt{2}, \\ \left|\chi_{\downarrow_{\mathrm{n}}1}\right\rangle &= \left(\sin\theta\left|\phi_{\downarrow_{\mathrm{e}}}\right\rangle + \cos\theta\left|\phi_{\uparrow_{\mathrm{e}}}\right\rangle\right)\left|\downarrow_{\mathrm{n}}\right\rangle/\sqrt{2}, \\ \left|\chi_{\downarrow_{\mathrm{n}}2}\right\rangle &= \left(\cos\theta\left|\phi_{\downarrow_{\mathrm{e}}}\right\rangle - \sin\theta\left|\phi_{\uparrow_{\mathrm{e}}}\right\rangle\right)\left|\downarrow_{\mathrm{n}}\right\rangle/\sqrt{2}, \\ \left|\chi_{\uparrow_{\mathrm{n}}2}\right\rangle &= \left(\left|\phi_{\downarrow_{\mathrm{e}}}\right\rangle - \left|\phi_{\uparrow_{\mathrm{e}}}\right\rangle\right)\left|\uparrow_{\mathrm{n}}\right\rangle/\sqrt{2}, \end{aligned} \tag{41}$$

where $\tan 2\theta = -\frac{1}{2}g_{\mathrm{e}}\mu_{\mathrm{B}}H_x/A$. The eigenenergies of the electron–nucleus system are

$$\begin{aligned} E_{\uparrow_{\mathrm{n}}1} &= -\frac{g_{\mathrm{e}}\mu_{\mathrm{B}}}{2}H_z - \frac{g_{\mathrm{n}}\mu_{\mathrm{n}}}{2}H_z - \frac{A}{4} - \frac{g_{\mathrm{e}}\mu_{\mathrm{B}}H_x}{2}, \\ E_{\downarrow_{\mathrm{n}}1} &= -\frac{g_{\mathrm{e}}\mu_{\mathrm{B}}}{2}H_z + \frac{g_{\mathrm{n}}\mu_{\mathrm{n}}}{2}H_z + \sqrt{\left(\frac{A}{4}\right)^2 + \left(\frac{g_{\mathrm{e}}\mu_{\mathrm{B}}H_x}{2}\right)^2}, \\ E_{\downarrow_{\mathrm{n}}2} &= \frac{g_{\mathrm{e}}\mu_{\mathrm{B}}}{2}H_z + \frac{g_{\mathrm{n}}\mu_{\mathrm{n}}}{2}H_z - \sqrt{\left(\frac{A}{4}\right)^2 + \left(\frac{g_{\mathrm{e}}\mu_{\mathrm{B}}H_x}{2}\right)^2}, \\ E_{\uparrow_{\mathrm{n}}2} &= \frac{g_{\mathrm{e}}\mu_{\mathrm{B}}}{2}H_z - \frac{g_{\mathrm{n}}\mu_{\mathrm{n}}}{2}H_z + \frac{A}{4} + \frac{g_{\mathrm{e}}\mu_{\mathrm{B}}H_x}{2}. \end{aligned} \tag{42}$$

Table 2. Change of the hyperfine and Zeeman splitting of the spin states of the donor electron.

H_z (T)	$\Delta_{\uparrow_{\mathrm{e}}}$ (μeV)	$\Delta_{\downarrow_{\mathrm{e}}}$ (μeV)	Δ_2 (μeV)	Δ_1 (μeV)
3.0	0.03	0.46	0.10	0.53
5.0	−0.11	0.61	−0.04	0.68
7.0	−0.25	0.75	−0.18	0.82

The oscillator strength for the exciton recombination in Si:P is $f = 7.1 \times 10^{-6}$ (see [17]). The binding energy of the exciton to the phosphorus donor is $E_{\mathrm{binding}} = 4.7$ meV. The recombination rate is about $w = 400\ \mathrm{s}^{-1}$. This leads to an interaction energy of

$$E_{\mathrm{int}} = \sqrt{\hbar w\Gamma} = 12\ \mathrm{neV}, \tag{43}$$

where $\Gamma = 100\ \mu$eV is the linewidth of the recombination.

Let us first investigate the ODMR method. If the electron–photon interaction energy E_{int} is much weaker than the microwave coupling energy $g_{\mathrm{e}}\mu_{\mathrm{B}}H_x$, the states $|\chi_{\uparrow_{\mathrm{n}}1}\rangle$, $|\chi_{\downarrow_{\mathrm{n}}1}\rangle$, $|\chi_{\downarrow_{\mathrm{n}}2}\rangle$, and $|\chi_{\uparrow_{\mathrm{n}}2}\rangle$ are good eigenstates. Then the ODMR method works, because the final state of the radiative recombination is given by $|\chi_{\uparrow_{\mathrm{n}}1}\rangle$, which doubles the lifetime of the bound exciton. In order to double the lifetime of the bound exciton in an experiment, the transverse microwave field should have a strength of at least $H_x = 1.0$ G, leading to a microwave coupling energy of $g_{\mathrm{e}}\mu_{\mathrm{B}}H_x = 10.0$ neV.

The calculations shown in equation (42) also reveal our second method for improving the resolution of the optical readout of a single nuclear spin, which is a frequency-resolved photon measurement. It can be seen from equation (42) that the hyperfine splittings are increased by means of the ESR field, which effectively increases the optical resolution. In order to obtain at least a 10% increase of the hyperfine + Zeeman splitting of the two lowest energy levels, the oscillating transverse magnetic field must have a strength of 10.0 G, which yields the transverse Zeeman splittings of the electron and nuclear spin of $g_{\mathrm{e}}\mu_{\mathrm{B}}H_x = 0.12\ \mu$eV and $g_{\mathrm{n}}\mu_{\mathrm{n}}H_x = 0.07$ neV, respectively. For a longitudinal magnetic field of $H_z = 3.0$ T, the shifted hyperfine splitting is $\Delta_2 = E_{\uparrow_{\mathrm{n}}2} - E_{\downarrow_{\mathrm{n}}2} = 0.10\ \mu$eV, whereas $\Delta_1 = E_{\downarrow_{\mathrm{n}}1} - E_{\uparrow_{\mathrm{n}}1} = 0.53\ \mu$eV. The shifted hyperfine and Zeeman splittings for $H_z = 3.0$, 5.0, and 7.0 T are shown in table 2.

Frequency-resolved photon detection has the advantage that only few photons need to be detected to determine the spin of the nucleus, whereas the ODMR measurement needs to be done in a time ensemble of photon measurements in order to determine the radiative recombination time. Maybe the hyperfine + Zeeman splitting of $\Delta_{\downarrow_{\mathrm{e}}} = A/2 + g_{\mathrm{n}}\mu_{\mathrm{n}}H_z = 0.75\ \mu$eV in a $H_z = 7.0$ T field is already sufficient for frequency-resolved photon detection.

7. Conclusion

We calculated the oscillator strength of recombination of an exciton bound to a donor electron in silicon. We showed that the Umklapp-assisted recombination, consisting of a Coulomb interaction between the electron of the bound exciton and the donor electron and the recombination of the virtually

excited electron with the hole, makes the main contribution. The calculation of the Umklapp-assisted recombination was done in second-order perturbation theory. We made use of the empirical pseudopotential method to find the Bloch wavefunctions of silicon. The calculated oscillator strength is in good agreement with the experiment. The Umklapp-assisted recombination of the exciton can be used to read out the spin state of the nucleus of a phosphorus donor. Therefore we also gave two methods to improve the resolution of the optical detection of the nuclear spin of a donor electron in Si:P.

Acknowledgments

We thank Marilyn Hawley, Geoff Brown and Holger Grube for useful discussions. This work was supported by LDRD from Los Alamos National Laboratory and the US NSF DMR-0403465. This research was supported in part by the National Science Foundation under grant no. PHY99-07949.

Appendix A. Bandstructure of silicon

We choose the empirical pseudopotential method to calculate the bandstructure of silicon [18–20]. A brief review of this method is given in appendix B. We need to solve the Schrödinger equation for the pseudowavefunction, i.e.

$$\frac{\hbar^2(\mathbf{k}+\mathbf{G})^2}{2m_e}u_{\mathbf{G}} + \sum_{\mathbf{G}'} V_0(|\mathbf{G}-\mathbf{G}'|)u_{\mathbf{G}'} = Eu_{\mathbf{G}}. \tag{A.1}$$

We diagonalize it using the 137 **G**-vectors shown in table 3 and the form factors $V_S(G=\sqrt{3}) = -3.049$ eV, $V_S(G=\sqrt{8}) = 0.750$ eV and $V_S(G=\sqrt{11}) = 0.985$ eV.

We calculate the bandstructure of silicon for 100 points in **k**-space in the direction of the X point. The bandstructure is shown in figure 1. For our Umklapp-assisted recombination the following symmetries are important: the conduction (valence) band at the Γ point has the symmetry $\Gamma_{25'}$ (Γ_{15}), which transforms as $\{yz, xz, xy\}$ ($\{x, y, z\}$). The conduction band at the X point has the symmetry Δ_1, which transforms as $\{z\}$. So the initial bound electron state before the recombination has the symmetry Δ_1 and the hole has the symmetry Γ_{15}. Since the spin–orbit splitting at the Γ point is $\Delta_{so} = 0.044$ eV (see [26]), the heavy-hole states including spin are represented by

$$\begin{aligned}
\left|J=\frac{3}{2};M=\frac{3}{2}\right\rangle &= \frac{1}{\sqrt{2}}\left(|yz\rangle + \mathrm{i}\,|xz\rangle\right)|\uparrow\rangle\,,\\
\left|J=\frac{3}{2};M=\frac{1}{2}\right\rangle &= \sqrt{\frac{2}{3}}\,|xy\uparrow\rangle - \frac{1}{\sqrt{6}}\,|(y+\mathrm{i}x)z\downarrow\rangle\,,\\
\left|J=\frac{3}{2};M=-\frac{1}{2}\right\rangle &= \sqrt{\frac{2}{3}}\,|xy\downarrow\rangle + \frac{1}{\sqrt{6}}\,|(y-\mathrm{i}x)z\uparrow\rangle\,,\\
\left|J=\frac{3}{2};M=-\frac{3}{2}\right\rangle &= \frac{1}{\sqrt{2}}\left(|yz\rangle - \mathrm{i}\,|xz\rangle\right)|\downarrow\rangle\,.
\end{aligned} \tag{A.2}$$

That is the origin of the selection rules found experimentally in [11].

Table 3. **G**-vectors used in the empirical pseudopotential calculation.

G	$\mathbf{G}^2$	Direction	No.	Sum
(000)	0	Γ	1	1
(111)	3	2L	8	9
(200)	4	2X	6	15
(220)	8	2K	12	27
(311)	11	2L + 2X	24	51
(222)	12	4L	8	59
(400)	16	4X	6	65
(331)	19	2L + 2K	24	89
(420)	20	2X + 2K	24	113
(422)	24	4L + 2X	24	137

Appendix B. Empirical pseudopotential method

We give here a brief review of the empirical pseudopotential method. At each lattice site there is an atom with a nucleus, core electrons and valence electrons. The attractive nuclear potential V_n is large and varies strongly throughout the lattice. The main observation is that V_n is almost canceled by the repulsive potential V_{rep} produced by the core electrons. So we need to consider only the valence electrons moving in a net weak one-electron potential V_p, which is called the pseudopotential.

The full Bloch wavefunctions can be expressed as

$$\Phi = \phi + \sum_t \alpha_t \varphi_t. \tag{B.1}$$

Φ must be orthogonal to the core wave functions φ_t, i.e. $\langle\varphi_t|\Phi\rangle = 0$, which yields

$$\alpha_t = -\langle\varphi_t|\phi\rangle\,. \tag{B.2}$$

Then applying the Hamiltonian $\mathcal{H}_n = p^2/2m_e + V_n$ to Φ leads to the Schrödinger equation

$$\left(\frac{p^2}{2m_e} + V_n + V_{rep}\right)\phi = E\phi, \tag{B.3}$$

where the short-range non-Hermitian repulsive potential is given by

$$V_{rep}\phi = \sum_t (E - E_t)\,\varphi_t\,\langle\varphi_t|\phi\rangle\,, \tag{B.4}$$

with E being the full energy eigenvalue of Φ. ϕ is called the pseudowavefunction. Since the crystal potential is periodic, the pseudopotential $V_p = V_n + V_{rep}$ and can be expanded in a Fourier series over the reciprocal lattice vectors **G**, i.e.

$$V_p = \sum_{\mathbf{G}} \tilde{V}_0(\mathbf{G})\mathrm{e}^{\mathrm{i}\mathbf{G}\cdot\mathbf{r}}, \tag{B.5}$$

where

$$\tilde{V}_0(\mathbf{G}) = \frac{1}{L^3}\int \mathrm{d}^3r\, V_0(\mathbf{r})\mathrm{e}^{-\mathrm{i}\mathbf{G}\cdot\mathbf{r}}. \tag{B.6}$$

For zincblende and diamond lattices a two-atom basis is usually chosen, such that

$$V_0(\mathbf{r}) = V_{cation}(\mathbf{r}-\tau) + V_{anion}(\mathbf{r}+\tau), \tag{B.7}$$

where $\boldsymbol{\tau} = (1, 1, 1)d/8$. Then the Fourier potential reads

$$\tilde{V}_0(\mathbf{G}) = \mathrm{e}^{\mathrm{i}\mathbf{G}\cdot\boldsymbol{\tau}}\,\tilde{V}_{\mathrm{cation}}(\mathbf{G}) + \mathrm{e}^{-\mathrm{i}\mathbf{G}\cdot\boldsymbol{\tau}}\,\tilde{V}_{\mathrm{anion}}(\mathbf{G}). \tag{B.8}$$

The Fourier coefficients can be rewritten in terms of the symmetric and antisymmetric form factors $\tilde{V}_S = \tilde{V}_{\mathrm{cation}} + \tilde{V}_{\mathrm{anion}}$ and $\tilde{V}_A = \tilde{V}_{\mathrm{cation}} - \tilde{V}_{\mathrm{anion}}$. Thus

$$\tilde{V}_0(\mathbf{G}) = \cos(\mathbf{G}\cdot\boldsymbol{\tau})\tilde{V}_S(\mathbf{G}) + \mathrm{i}\sin(\mathbf{G}\cdot\boldsymbol{\tau})\tilde{V}_A(\mathbf{G}), \tag{B.9}$$

where the prefactors of the form factors are the structure factors. Since silicon has a diamond lattice, $\tilde{V}_A(\mathbf{G}) = 0$.

The pseudowavefunction can also be expanded in a Fourier series, i.e.

$$\phi(\mathbf{r}) = \mathrm{e}^{\mathrm{i}\mathbf{k}\cdot\mathbf{r}}u(\mathbf{r}) = \mathrm{e}^{\mathrm{i}\mathbf{k}\cdot\mathbf{r}}\sum_{\mathbf{G}} u_{\mathbf{G}}\mathrm{e}^{\mathrm{i}\mathbf{G}\cdot\mathbf{r}}. \tag{B.10}$$

Inserting the pseudowavefunction ϕ and the pseudopotential V_{p} into equation (B.3) yields

$$\frac{\hbar^2(\mathbf{k}+\mathbf{G})^2}{2m_{\mathrm{e}}}u_{\mathbf{G}} + \sum_{\mathbf{G}'} V_0(|\mathbf{G}-\mathbf{G}'|)u_{\mathbf{G}'} = Eu_{\mathbf{G}}. \tag{B.11}$$

Diagonalization of this Hamiltonian yields an effective mass Hamiltonian of the form $\mathcal{H}_{\mathrm{eff}} = p^2/2m^*$, which determines the bandstructure shown in figure 1.

References

[1] Ziese M and Thornton M J 2001 *Spin Electronics* (Berlin: Springer)

[2] Awschalom D D, Loss D and Samarth N 2002 *Semiconductor Spintronics and Quantum Computation* (Berlin: Springer)

[3] Loss D and DiVincenzo D P 1998 *Phys. Rev.* A **57** 120

[4] Kane B 1998 *Nature* **393** 133

[5] Kroutvar M, Ducommun Y, Heiss D, Bichler M, Schuh D, Abstreiter G and Finley J J 2004 *Nature* **432** 81

[6] Dutt M V G, Cheng J, Li B, Xu X, Li X, Berman P R, Steel D G, Bracker A S, Gammon D, Economou S E, Liu R-B and Sham L J 2005 *Phys. Rev. Lett.* **94** 227403

[7] Fu K-M C, Ladd T D, Santori C and Yamamoto Y 2004 *Phys. Rev.* B **69** 125306

[8] Brossel J and Bitter F 1952 *Phys. Rev.* **86** 308
van Kesteren H W, Kosman E C, Greidanus F J A M, Dawson P, Moore K J and Foxon C T 1988 *Phys. Rev. Lett.* **61** 129
Köhler J, Disselhorst J A J M, Donckers M C J M, Groenen E J J, Schmidt J and Moerner W E 1993 *Nature* **363** 242
Wrachtrup J, von Borczyskowski C, Bernard J, Orrit M and Brown R 1993 *Nature* **363** 244

[9] Berman G P, Doolen G D, Hammel P C and Tsifrinovich V I 2001 *Phys. Rev. Lett.* **86** 2894

[10] Berman G P, Brown G W, Hawley M E and Tsifrinovich V I 2001 *Phys. Rev. Lett.* **87** 097902

[11] Sauer R and Weber J 1976 *Phys. Rev. Lett.* **36** 48

[12] Kirczenow G 1977 *Solid State Commun.* **21** 713

[13] Chang Y C and McGill T C 1980 *Phys. Rev. Lett.* **45** 471

[14] Chang Y C and McGill T C 1982 *Phys. Rev.* B **25** 3945

[15] Lightowlers E C, Henry M O and Vouk M A 1977 *J. Phys. C: Solid State Phys.* **10** L713

[16] Pfeiffer R S and Shore H B 1982 *Phys. Rev.* B **25** 3897

[17] Dean P J, Flood W F and Kaminsky G 1967 *Phys. Rev.* **163** 721

[18] Cohen M L and Bergstresser T K 1966 *Phys. Rev.* **141** 789

[19] Chelikowsky J R and Cohen M L 1974 *Phys. Rev.* B **10** 5095

[20] Chelikowsky J R and Cohen M L 1976 *Phys. Rev.* B **14** 556

[21] Bolivar P H, Brucherseifer M, Rivas J G, Gonzalo R, Reynolds A L, Holker M and de Maagt P 2003 *IEEE Trans. Microw. Theory Tech.* **51** 1062

[22] Ashcroft N W and Mermin N D 1976 *Solid State Physics* (Belmont, MA: Brooks Cole)

[23] Hawley M, Brown G and Grube H 2005 private communication

[24] Kohn W and Luttinger J M 1955 *Phys. Rev.* **98** 915

[25] Koiller B, Hu X and Das Sarma S 2002 *Phys. Rev. Lett.* **88** 027903

[26] Bassani F, Iadonisi G and Preziosi B 1974 *Rep. Prog. Phys.* **37** 1099

[27] Cohen-Tannoudji C, Diu B and Laloë F 1977 *Quantum Mechanics* (New York: Wiley)

[28] Stoneham A M 1975 *Theory of Defects in Solids* (Oxford: Clarendon) p 886

[29] Cohen-Tannoudji C, Dupont-Roc J and Grynberg G 1992 *Atom-Photon Interactions* (New York: Wiley)